

**Astrophysics and Technical Study of a Solar Neutrino Spacecraft
NASA 2018 NIAC Phase-1 Grant Final Report
Grant #80NSSC18K0868**

**N. Solomey (PI), C. Gimar, A. Nelsen, M.L. Buchele, H. Meyer
Wichita State University, Kansas**

**R. McTaggart
University of South Dakota**

**Mark Christl
NASA MSFC NSSTC, Huntsville, Alabama**

Executive Summary:

We report on our study of the design of a neutrino detector, shielding and veto array needed to operate a neutrino detector in space close to the Sun. This study also took into account the expected rates of Galactic gamma and cosmic rays in addition to the particles from the Sun. These preliminary studies show that we can devise a detector such that a small signal of neutrino interactions can be extracted from a large random number of events from the background sources using a double timing method from the conversion electron produced in the neutrino interaction and a secondary delayed signal from the nuclear excited state produced from the initial neutrino interaction; in our case the conversion of Ga 69 or 71 into Ge 69 or 71, but this method could apply to other nuclei with large neutrino cross sections such as Ir 115.

Although these types of events need to be above 0.405 MeV neutrino energy and are only 66% of all conversion neutrino interactions on Gallium, this is a small price to pay for an increase of 10,000 by going close to the Sun to enhance the neutrino rate over the background combinatorial fake-signal events. The conclusion of this Phase-1 study is very positive in that we can get the backgrounds less than 20% fake signals, and in addition to this we have devised another shielding method that makes the Galactic gamma-ray rate a hundred fold less which will make further improvements over these initial estimates. Although these studies are very encouraging it suggests that the next step is a NIAC Phase-II to actually build a test device, measuring basic principles such as light attention within the scintillator with high dopants and to take data in the lab with a cosmic-ray test stand and triggered X-ray source for comparison with simulated expected performance of the detector. This would be the perfect lead into a future proposal beyond a NIAC Phase-II for a test flight of a small one pint detector in orbit of the detector concept beyond Earth outside of the radiation belts.

Introduction:

The Sun provides all of the energy that our planet needs for life and has been doing so for five billion years. Understanding our Sun and its interior is one of the major goals of the NASA Science program. Still this is a very difficult task because very little makes it directly out of the Sun's interior. The energy we see today, that warms the Earth, was made 50,000 to 80,000 years ago and is only now coming to the surface to make light. However, neutrinos penetrate matter almost without interaction and make it to Earth in only eight minutes from creation. Since neutrinos interact only weakly they are hard to detect; never-the-less within the last ten years neutrino detectors on Earth have started to reliably detect neutrinos from the fusion reactions in the interior of the Sun and scientists have started to use this information to investigate the Sun's nuclear furnace.

Changes in solar neutrino flux make it advantageous to take a neutrino detector into space since the solar neutrino intensity changes dramatically as the inverse square of the distance from the Sun, by five orders of magnitude when going from the Earth to the Sun or from the Earth to the current position of the Voyager 1 space craft (**Table 1**). Launch of a neutrino detector into space toward the Sun will: a) aim to significantly reduce the required detector size and experimental costs while allowing for improved detector energy resolution and performance, b) attempt to completely eliminate background terrestrial neutrino sources for improved measurement accuracy, and c) conduct unique science experiments near the Sun not achievable with much larger detectors on the Earth.

NASA's interest in deep space exploration has been a key factor in its unmanned spacecraft development and launch of exploration science satellites and spacecraft. NASA has done exceptional experiments in space where science benefits from the unique platform of spacecraft that provides unprecedented views. For example the Hubble Space telescope is really a small and very common instrument, but when it is put into an orbit high above the Earth, it becomes one of the most powerful optical observatories man has ever made. Moving neutrino observations to space is the next obvious step.

The concept of putting a neutrino detector in close orbit of the sun is completely unexplored and innovative. Its scientific return is to vastly enhance the understanding of the solar interior which is a NASA major goal as stated in the decadal survey. Preliminary calculations show that such a spacecraft if properly shielded, can operate in this environment both taking data of neutrino interactions which can be distinguished from random background rates of solar Electromagnetic emissions, Galactic charged cosmic-ray and gamma-rays by using a double pulsed signature. The idea of using a Heavy Liquid Scintillator where the CH₂ has all the Hydrogen atoms changed to Deuterium would give sensitivity to multiple neutrino type of interactions. If successful this spacecraft concept will enable a whole new type of mission to explore and study our Sun, in details that could not be done with the largest neutrino detectors on Earth nor other type of space-craft measurements that are not using neutrino detection.

Table 1: Intensity of solar neutrinos at various distances from the Sun.

Distance from Sun	Solar Neutrino intensity relative to Earth
696342 km	46400
1500000 km (~3 Sun R)	10000
4700000 km (~7 Sun R)	1000
15000000 km	100
474340000 km	10
Mercury	6.7
Venus	1.9
Earth	1
Mars	0.4
Astroid belt	0.1
Jupiter	0.037
Saturn	0.011
Uranus	0.0027
Neptune	0.00111
Pluto	0.00064
KBP	0.0002
Voyager 1 probe 2017	0.00006

Preformed Work:

This NIAC Phase-I grant provided start-up funding for nine months to study this new and innovative neutrino Solar project (vSOL) idea. The two-pronged research includes both science studies and a new innovative technology study for use in a future neutrino mission to the Sun.

Science Studies: Four areas will be studied: 1) Solar physics - the study of the nuclear furnace in the interior of the Sun, which includes understanding what exposure would be necessary to see the CNO cycle neutrinos for the first time. 2) Particle physics that can be studied with the solar neutrinos generated, 3) Nuclear Physics matter effects on neutrino propagation and 4) Dark Matter studies. Current theories focus on the Standard Solar Model on the location radius of nuclear fusion in the Sun's core. It is known that all of the Sun's energy comes from nuclear fusion reactions in the Sun's core, but there remain many unanswered questions in stellar evolution and astrophysics that can be addressed with a close solar orbiting spacecraft equipped with a neutrino detector. These are: a) solar fusion reaction neutrino spectrum, b) size and shape of the nuclear fusion reaction core in 3D, c) nuclear fusion rates of rare processes, and d) changes of the nuclear fusion reactions over time and regions within the Sun. With a close orbiting satellite, these studies could be expanded due to a larger event rate. For a satellite out of the ecliptic plane, views of the nuclear fusion core from various solar latitudes could allow for a 3D image of the fusion core. There are two categories of nuclear physics studies that can be performed with solar neutrinos and a spacecraft detector in near orbit of the Sun. These are studies of the matter effect on neutrino propagation through solar material and rare nuclear isotope fusion. Because the Sun is a rotating ball of gas, the Sun itself has an equatorial bulge

much the like the Earth. Neutrinos produced in nuclear fusion processes within the solar core propagate through different amounts of matter for the equatorial view and polar view. Theoretically, it should be possible to study this effect by placing a satellite in an orbit around the Sun that is not in the ecliptic plane. Also, due to the near solar orbit of the satellite, the detector will be more sensitive to the higher mass fusion processes of heavy isotopes that reside in the solar core than solar neutrino detectors located on the Earth. Both of these studies are specific only to a space-based neutrino detector and cannot be performed by experiments located on the Earth. Particle Physics can use this data for the study of neutrino oscillations, and inside the 35 solar Radii limit the neutrinos are de-coherent and this would tell us the unique science of particle physics oscillation.

An indirect search for Dark Matter in the core of the Sun can also be a result of such an experiment. Imagine that Dark Matter has accumulated in the gravitational well formed by the large mass of the Sun. This would distort the observed nuclear fusion region, displacing the neutrino source from the current calculations without any dark matter and making for a way to not only identify if Dark Matter is in the core of the Sun, but also would allow for a way to measure how much Dark Matter has accumulated in the Sun's core.

The first step to study these ideas is to create a detailed physics simulation. Initial simulations of a simple detector have begun but they will be influenced by the science studies to be carried out and the needs of these science studies on the technical detector development.

Technical Development Studies: Development of technology suitable for space flight is of major importance since none of the techniques currently used in ground-based solar neutrino detectors have been verified for space flight. Given that the potential science returns as reviewed above, laboratory-based testing and development of detector technology for these missions is needed, **Table 2** summarizes possible neutrino interaction modes. Detector technology for neutrinos are well established but by NASA standards are not flight ready technology. This early stage proposal aims to study the science and detector technology using simulations but not construction of any lab tests. The goal of this study will advance the technical space flight readiness level by determining which of the many possible detectors should be pursued to ready them for space flight technical readiness based upon which detector technology performs the best in simulation studies. This NIAC goal can be achieved in a short time and with review by NASA the research team should be able to find the best method to flight evaluation.

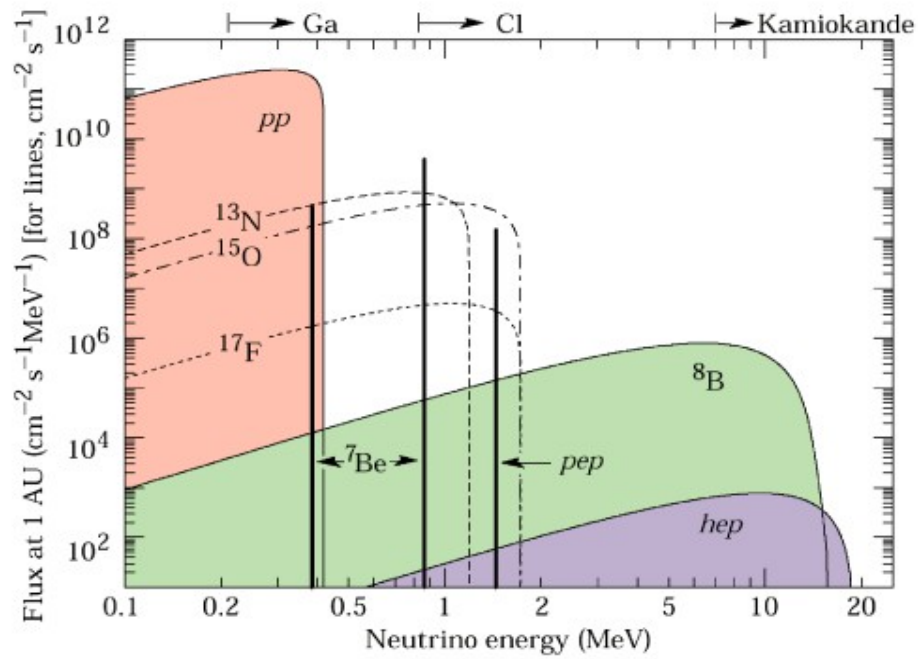


Figure 1: Neutrino emissions expected from Solar Nuclear fusion [1].

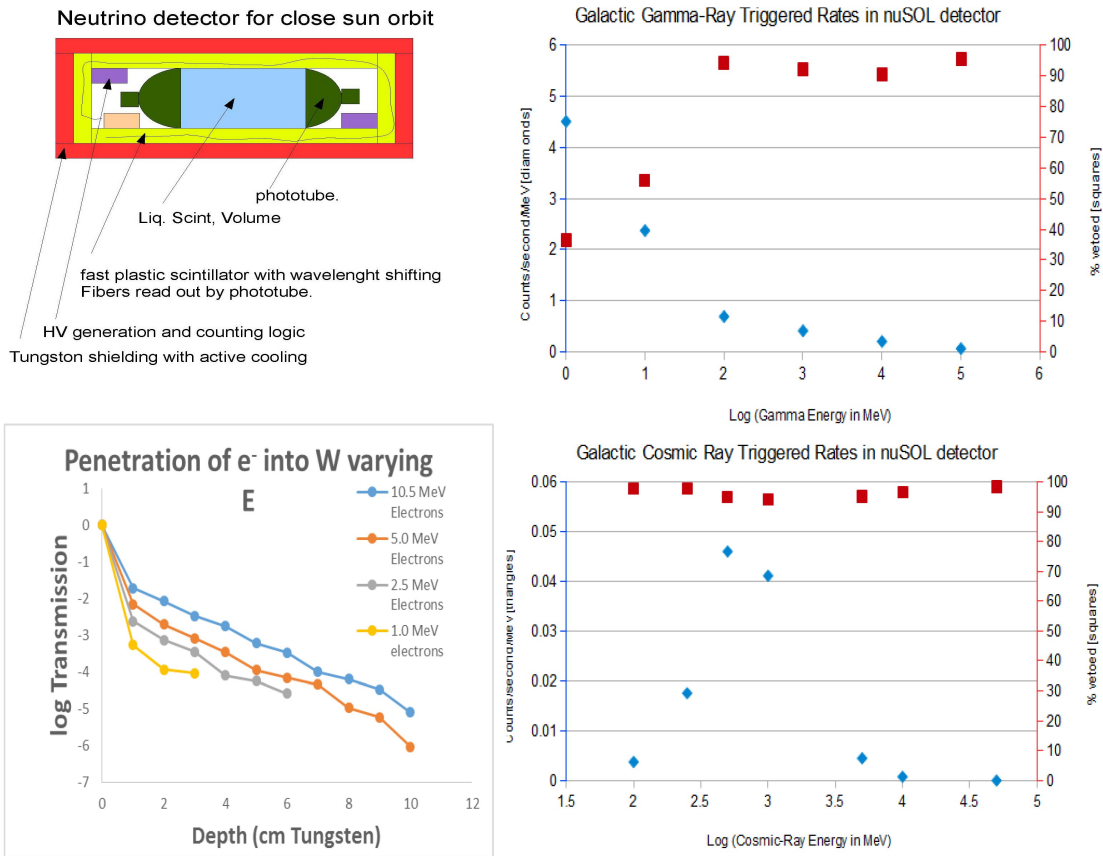


Figure 23: Top left: sketch of detector, Top right, Galactic Gamma-ray rates simulated, Bottom right Galactic Cosmic-Ray rate simulated and Bottom Left shield to stop solar EM Radiation.

An important aspect of this design study that can be answered with simulations is the different rates from backgrounds and the proper shielding needed. Measurements from the Helios 1 Probe that the charged protons went up to 200 MeV but had an extremely small rate of $10^{-2} \text{ (cm}^2 \text{ sr s MeV)}^{-1}$ and Helios 2 electron spectrum went up to only 20 MeV [1] shown in **Figure 1**. A simple first detector idea is shown in **Figure 2** upper left. A preliminary Monte-Carlo simulation of this detector was performed for this study, see **Figure 3**. With the axis of the cylindrical volume pointed towards the sun and behind a sunshade, the positrons produced from 1.8 MeV neutrinos off of hydrogen and had a track length of 0.83 cm with higher energy neutrinos at 9 MeV producing longer tracks of 4.4 cm. These electron tracks and annihilation photons in the liquid scintillator were 96% contained in the sensitive volume for solar neutrinos up to the 18 MeV energy. In a final space-craft the Sun shade would also serve as an Electromagnetic shower shield (see **Figure 2** lower left), and estimated neutrino count rates are in **Table 3** comparing a present day experiment to a 250 kg satellite close to the Sun.

Present methods of neutrino detection are aimed at large detector volumes [2], but when a small detector volume can be used in an environment where the rates are 4 orders of magnitude larger than other techniques can be employed. The first method is to replace the H in Liquid

Scintillator with D using a 100% complete Catalytic process and have the neutrino capture on D into ^2He which decays into two signals and a second simultaneous method is to dope the scintillator such as with Ga to look for the neutrino capture into Ge m1 or m2 excited state that decays 2 to 5 micro-seconds into the Ge ground state emitting signature X-rays, see **Table 2**. Another method is the neutrino capture on ^{12}C into ^{12}N and a ms secondary decay process, which has the advantage of being blind to solar neutrino and would only be sensitive to larger energy neutrinos as part of the Astrophysics mission such a space-craft would also perform in orbit. All three of these methods would cover a broad range of neutrino energies and have a double signal to separate out the signal from background. Simulations of this detector have been done and show the rates for Galactic Cosmic rays and Solar Electromagnetic radiation very acceptable.

Interaction Mode	2 nd signature	Timing	Energy	ν energy threshold
$^{12}\text{C} + \nu$ into $e^- + ^{12}\text{N}$	^{12}N decays into $^{12}\text{C} + e^+$	11 ms	e+e- annihilation 2.2 MeV signature	15 MeV
$\text{Cl} + \nu$ into $e^- + \text{Ar}$	Chemical sniffing			0.85 MeV
$^{18}\text{O} + \nu$ into $e^- - ^{18}\text{F}$ m1	^{18}F m1 decays into ^{18}F and gamma	162 ns	1121 keV	7 MeV
$^{69}\text{Ga} + \nu$ into $e^- - ^{69}\text{Ge}$ m1 or m2	^{69}Ge m1 decays X-ray	5 us	86 keV	0.405 MeV
	^{69}Ge m2 decay gamma	2.8 us	397 keV	0.491 MeV
$^{71}\text{Ga} + \nu$ into $e^- - ^{71}\text{Ge}$ m1	^{71}Ge m1 decay gama	20 ms	175 keV	0.94 MeV
$\text{D} + \nu$ into $e^- - ^2\text{He}$	^2He decays to proton proton Topology of event	<1 ns	back to back protons depends on neutrino energy	2.2 MeV

Table 2: Solar Neutrino interaction mode, subsequent decays, timing and energy threshold for reaction.

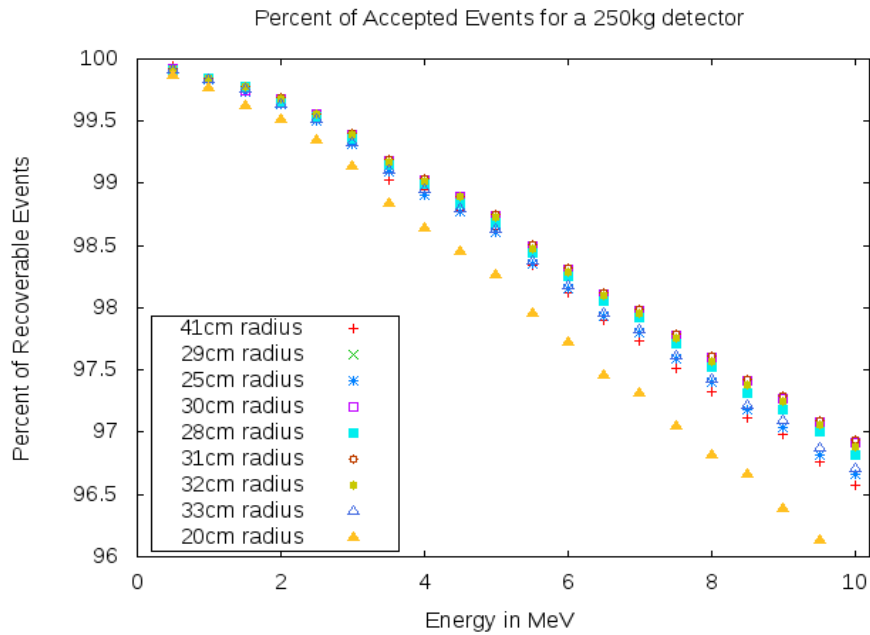


Figure 4: Acceptance of 250 kg Neutrino detector from 0.1 to 10 MeV energy for different radii of the cylinder.

Galactic gamma ray rates seen by Egret and Fermi satellite are reasonable to manage at $10^{-4}/\text{s cm}^2 \text{ sr}$. Solar neutrino detection rates are expected to be ten per hour, and through the double coincident in time will be identified in subsequent data analysis. Keeping the background low by both shielding and active veto will be the two ways to reduce these rates. Our simple simulation using these known rates, particle fluxes from Galactic sources and a rough design of the spacecraft neutrino detector are shown in **Figure 2** and support these first conclusions. The detector must live with a high rate of Galactic Cosmic Rays, High Energy Gamma Ray, and solar EM and protons some of which are shielded by the heat shield and outer container. In the simplest idea of the electronics each channel is stored in a time delay buffer. If a background event goes through after the first neutrino interaction signal is observed and before the second energy signature event then this event may be kept alive because the buffer streams of the photo-tube on the liquid scintillator can identify the background event with the same timing from the veto array observed event of either a GCR entering and exiting the liquid scintillator or a High Energy Photon interaction in either the veto array or the liquid Scintillator and then the shower exits the liquid scintillator producing a signal in the veto array. For the long lived processes of C-12 where the half-life of the processes is milliseconds then this is essential to keep the live time high and may even need to reject multi cosmic-ray background events, but it is also helpful for the micro-second decays of the Ga dopant options. For the timing signature see **Figure 4**. The electronics can also be improved by being sensitive to the 2nd decay which should have a characteristic pulse height of their respective decays.

It is expected that the electronics board would then provide all the signal process of the photo-tube signals of the detector volume and veto array and produce candidate events for neutrino interactions and background event readout converted to digital format and sent to the spacecraft's main computer for data storage and transmission. It is necessary for this board to also monitor live-time and different characteristic rates of backgrounds although the background trigger rate might be too hard to read out all of the events but we need to monitor the number of

these different types of background events and to provide some scaled down events for readout and later analysis. The electronics board needs to be able to be programmed by the spacecraft computer during flight if changes are necessary and in the event that different neutrino processes are used and the ability to set the decay half-life the pulse height of the signature signal events and to be able to handle multiple processes during the testing and flight of the detector. Also as the experiment progresses in flight it might be deemed necessary to change parameters so these need to be programmable and set, as well as reading out time stamps. It must be noted that once leaving near earth orbit the only clock for timing will be that on the electronics board so it must be of high accuracy. Although the first module produced for the lab test detector might not succeed some options to consider including are multiple background event rejection or rejection of isolated second pulses that do not meet the pulse height signature but still keeps the event alive for processing.

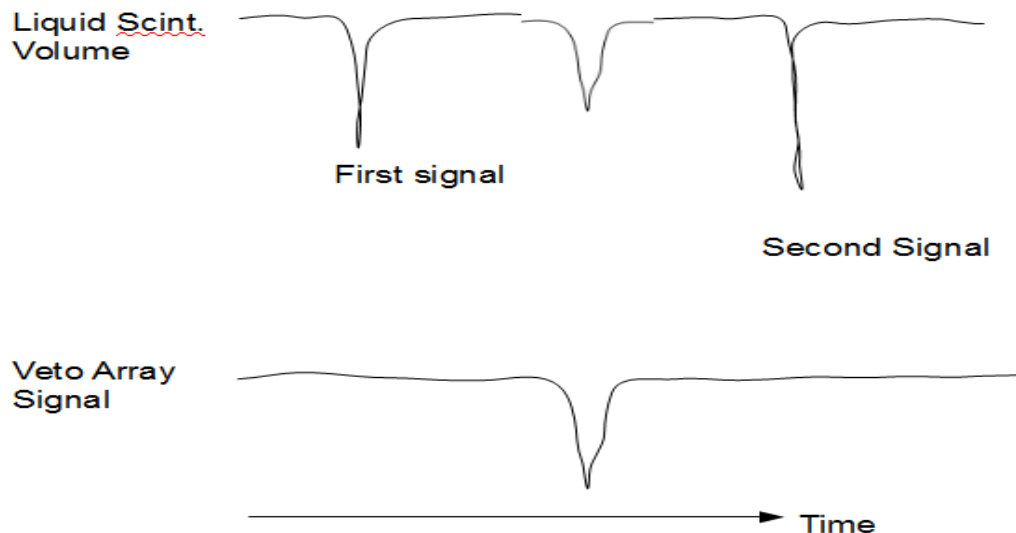


Figure 5: Top trace is the photo-tube pulse height of a neutrino interaction event in the Liquid Scintillator two pulses with a event inserted between the two signals from a background event. The bottom trace is the pulse height from the veto array photo-tube.

A small 250 kg active detector would be expected to perform ten times better than a 300 Ton detector on Earth, shown in **Table 3**. The main source of count rate in the detector will be that from solar electromagnetic radiation emission from the Sun, Galactic Gamma Rays and Galactic Cosmic Rays. This is expected to be in the region of 0.5 to 10 MeV and at 10 down to 10^{-1} counts/s cm^2 sr, again as previously seen by the Helios space craft. These researches have conducted an initial simple study of the shielding needed for such a spacecraft, but the final optimized shielding will be determined by the physics needs. A simulated cosmic-ray background event using a simple straw-man Geant-4 simulation design is shown in **Figure 5**. One of the best methods for solar neutrino detection is the conversion of solar neutrinos on Deuterium, often used by having a sack of heavy water. However, the process of making “heavy liquid scintillator” is a known process from 73 years ago the idea was created where Deuterium gas is infused into any Oil compound and with the help of a catalysts it is possible to have a 100% complete

replacement of all the Hydrogen into Deuterium. Although such a detector has never been made for neutrino or particle physics, the process is relatively simple and 100% complete and is part of this researcher's future planned studies.

Through an initial "back of the envelope" study (simple simulation program) we have reached the conclusion that the rates of particles in the detector from the direct Solar emissions and Galactic backgrounds from Cosmic-ray and Gamma-rays are reasonable, because they can be shielded or vetoed with advanced processing. Further detailed studies would have to prove this thoroughly. In addition to this these rate studies, so far we have also shown how a new technical method of detecting solar neutrinos can be done with "Heavy Liquid Scintillator" where a 100% complete method of changing the hydrogen to Deuterium is possible. We have laid out the design specifications for a signal and veto processing board for neutrino event selection, and how it would be used for background rejection and live time monitoring. All of these will need detailed simulation studies and to be matched to science needs as part of the proposed project. Sides benefits of such a final mission is that it would study ways to get closer to the Sun for possible future missions to distant stars using a slingshot effect or other science needs.

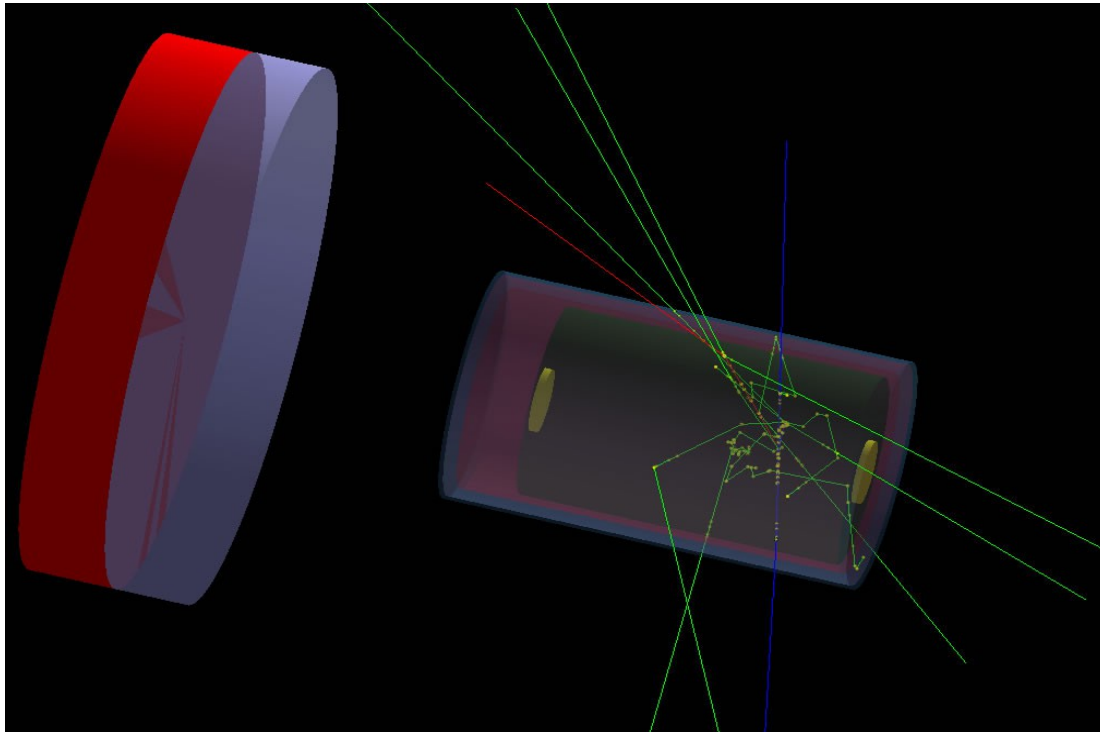


Figure 6: Simple first straw-man design of neutrino solar detector with a 50 GeV cosmic ray going through the veto and detector volume.

Neutrino Energy	300 ton Borexino	250 kg ν SOL at 7 R_{\odot}
0.4 – 0.8 MeV	15 ν /day	150 ν /day
0.8 – 1.5 MeV	3.5 ν /day	35 ν /day
>1.5 MeV	0.5 ν /day	5 ν /day

Table 3: Neutrino rates observed in the 300 ton Borexino detector on Earth and a 250 kg ν SOL detector at 7 solar Radii, for three intervals of neutrino energy.

Fast Timing simulations of Events with Backgrounds:

Outlined in the following section are the methods and results of efforts to simulate the particle signals produced in the proposed solar neutrino spacecraft. An emphasis of these efforts has been to isolate double-pulse signals associated with primary electrons and the following secondary photons from neutrino interactions with gallium nuclei. Progressive refinements of these simulations have thus far confirmed the plausibility of the detection scheme outlined in this report.

The primary challenge of this detector concept is separating the signals associated with the neutrino interaction products from other signals resultant of background particles. In the simulations described here, three sources of charged particles have been addressed: neutrino interaction products, galactic gamma-rays, and galactic cosmic rays. Currently, the neutrino detections are the result of the following interactions with gallium:

All of these interactions initially produce an electron and an excited germanium nucleus, of which the electron will produce a detectable light pulse in the liquid scintillator. Depending on the energy of the incoming neutrino, the interaction cross-section associated with each possible interaction, and the isotope of gallium involved, three possible secondary decay modes can occur as listed in the comma-delimited part of the given equations. These secondary decay modes take the excited germanium nucleus (represented by the “m1” or “m2” next to the atomic mass in the notation) to the ground state and result in the release of a detectable gamma-ray or x-ray. For these interactions, the emission of both an electron and photon in sequence proves advantageous to their detection amongst background particle events: the combination of the secondary photon’s specific energy value and the timing of the related decay allow for the associated signals to be pinpointed in comparison to dramatically uncharacteristic background signals. In constructing this simulation, attention was given to accurately replicating the energy and half-life characteristics (Table 1) of these decay events.

Decay Type	Half-Life	Emitted Photon Energy
Ge-69 m1 Decay	5 μ s	86 keV
Ge-69 m2 Decay	2.8 μ s	397 keV
Ge-71 m1 Decay	20 ms	175 keV

Table 1: Half-lives and photon energies of germanium decay events.

An accurate neutrino frequency and energy spectrum component of the simulation has been a more challenging aspect, and as of this writing continues to be optimized. Appropriately characterizing these aspects requires a combination of expectations based off of the standard solar model and the assumed capabilities of the detection scheme; however, both of these dependencies are open to large uncertainties. Thus, it is prudent to base these characteristics upon existing neutrino experiments utilizing similar methods. Considering that the proposed detector uses scintillation effects to detect the neutrino interaction products, it has been decided that a good reference for performance is the Borexino experiment. Although the GALLEX/GNO and the Soviet-American Gallium Experiment projects similarly use gallium interactions, the radiochemical detection of converted germanium nuclei for detection as opposed to scintillation methods in these experiments make their performance characteristics too dissimilar for adequate comparison [1][2]. Despite the different interaction scheme—neutrino-electron scattering—monitored in Borexino, the interactions observed are similar enough that the more pertinent consideration is given to the actual particle counting method [3]. To obtain a reasonable estimate (Table 2) on the observable neutrino flux, the predicted performance of Borexino has been scaled relative to the volume of the simulated detector, the energy threshold of the detectable interaction, and the distance of the simulated detector from the Sun.

Neutrino Energy Range	Borexino Predicted Rate (neutrios per day)	250 kg Simulated Detector at 7 Solar Radii (neurinos per day)
0.4 to 0.8 MeV	15	150
0.8 to 1.5 MeV	3.5	35
> 1.5 MeV	0.5	5

Table 2: Scaled rates for the simulated detector compared to adapted predictions from Borexino. [3]

Galactic gamma-ray and galactic cosmic ray rates for this simulation are obtained from the separate Geant4 simulations described elsewhere in this report. It should be noted that all of the values for background particles used here are after the application of the veto array component. Since this aspect of the Monte Carlo code is based upon older Geant4 simulations, the energy distribution of non-vetoed particles and the performance characteristics of the simulated veto array for these older simulations are given (Figure 1) for reference.

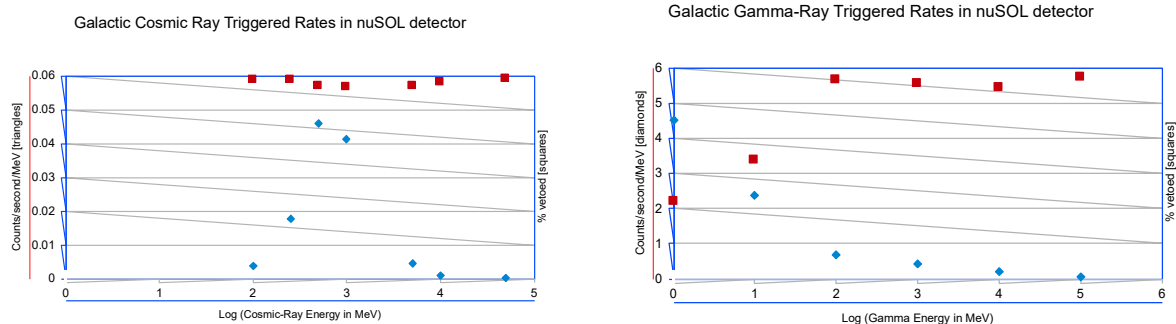


Figure 1: Original veto array performance characteristics and admitted particle energy distributions from Geant 4 simulations.

The heart of Monte Carlo simulations is the ability to produce random numbers that are at least in some minimal sense “random.” Since any means of producing numbers via computational methods will suffer from some kind of cyclic tendency and/or numerical instability, random number generator programs are more often considered “pseudo-random” in their abilities. For this project, accurately simulating naturally random occurrences of particle detections requires a pseudo-random number generator that is as least “pseudo” as possible. Early in this project, the random number generation functions available in standard C++ packages proved unsuitable for use; they produce values which fall into a regular pattern of magnitude and will generally avoid generating numbers very near zero or one. For these reasons, the MIXMAX family of pseudo-random number generators have been utilized here. Based off of Ansov C-systems—a mathematical function group with useful instabilities in their structure—this family of generators allows for the most random numerical output in the shortest computational time [4].

A basic consideration of this detector design is the rate at which the phototube electronics read the events in the scintillator volume. In other terms, what is the time window for a particle event to be read in the detector? An early, highly conservative approach was to use readout bins with a span of 100 nanoseconds; however, this was more for ease of development during initial coding. Considering the current state of particle detection technology, a much shorter time window can easily be accomplished. Thus, a more appropriate bin size is 10 nanoseconds, which has been used for all trials conducted since September.

It is now possible to give an overview of the working process of the Monte Carlo code constructed. First and foremost, the code “makes” event windows: a certain length of simulation time is specified and a loop is initiated for which each cycle of the loop corresponds to a sequential 10-nanosecond bin, continuing until the total time represented by all completed loop cycles equals the input time. In each cycle and for each possible particle outcome therein, a random number is generated and compared to a selected range of numbers within the probability associated with the particle outcome in question. If the random number is in the range, an appropriate particle event is registered as taking place in the time window. Since the number of windows in a single day of data collection exceed 8 trillion, the probability of a neutrino being detected in any single time bin is exceptionally low; hence the need for a very capable pseudo-random number generation method. Other particle events, though more probable, are still

relatively infrequent in comparison. When a particle event happens, a similar number comparison process is used to assign an energy value to the particle detected. For neutrino events, the initial energy value is actually that of the conversion electron emitted when a neutrino interacts with a gallium nucleus, and this energy assignment is in turn followed by additional steps to determine if and when the resultant germanium nucleus decays. When such a decay takes place, an x-ray or gamma-ray is generated in accordance with the initial state of the germanium nucleus. Each time bin containing an event is recorded in a text file which contains three columns: the bin number, a four-digit binary identifier of the particle event(s), and the energy value of the event(s).

To simulate the process of finding neutrino events, a “toy” detector code is applied to the data file from the Monte Carlo. The use of “toy” here is meant to emphasize that it is merely a way of testing the ability to isolate possible neutrino-related signals and not a final—or even recommended—algorithm for this purpose. It simply looks for events in close succession that fall in the right time range and energy values to possibly be the neutrino-related double-pulse signals, then examines the events’ binary codes to determine which are true detections or not. Another code is often applied which collects basic statistics, e.g. number of overall events, number of each kind of event, etc.

Initial testing of this code focused on its ability to produce the expected number of events, to replicate the energy spectrum of each event type, and to simulate the timing of the germanium decays. This last point—the germanium decay timings—represents the most consequential of these tests, as the true functionality of this Monte Carlo simulation rests with its ability to inherently reproduce exponential decay behavior. This overview will use as its test result example the October 29th, 2018 data run which simulated five days of detector operation.

Given first are the results for galactic gamma-rays (Figure 2) and cosmic rays (Figure 3) as compared to the expected distribution as programmed. Though the code was designed off of the Geant4 simulations for these values, the original simulation data for the gamma-rays used energy bins which were larger than the desired precision for the Monte Carlo code; hence, the Geant4-provided distributions were reparametrized for smaller energy bins. Here, the distributions for the example run have been plotted in bin sizes identical to the Geant4 originals. It is evident from these comparisons that the code is able to replicate these distributions proficiently.

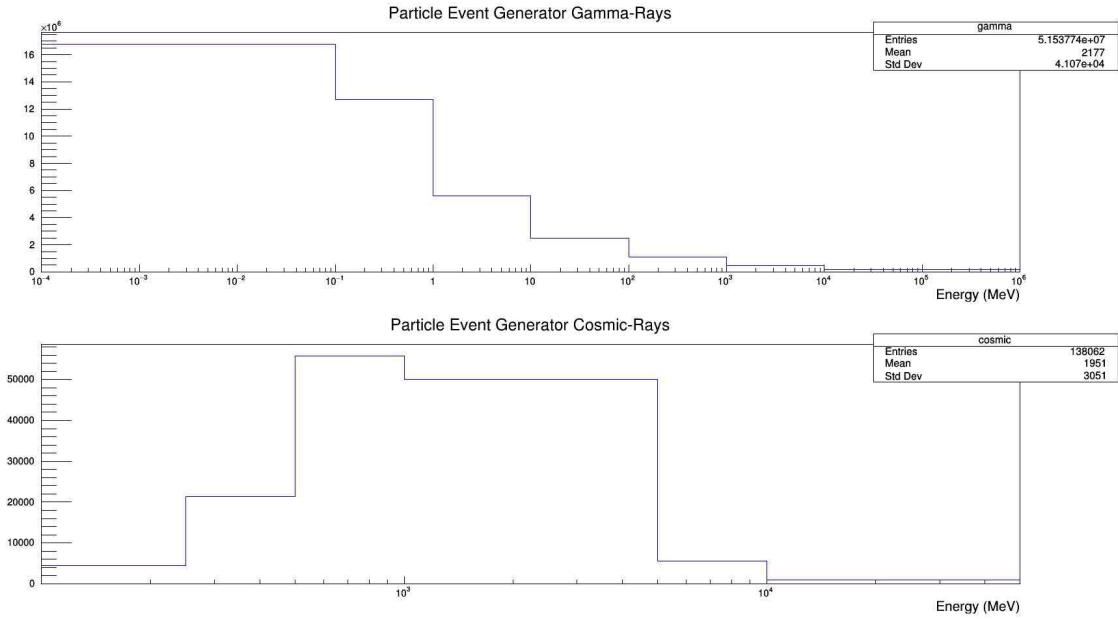


Figure 2 and Figure 3: Energy distributions of non-neutrino detection particles in the simulation.

Compared distributions for the neutrino energy spectrum are given in Figure 4 and the decay timing results given in Figure 5. Again, the energy spectrum results had to be reparametrized for the purposes of this project, albeit off of very rough assumptions. At this time, the energy distribution was derived from a functional fit to the expected Borexino-based neutrino counts. In future implementations, this will be corrected for the real observations from Borexino and the predictions of the Standard Solar Model. As with the galactic gamma-ray and cosmic ray results, the Monte Carlo holds to the expected behavior.

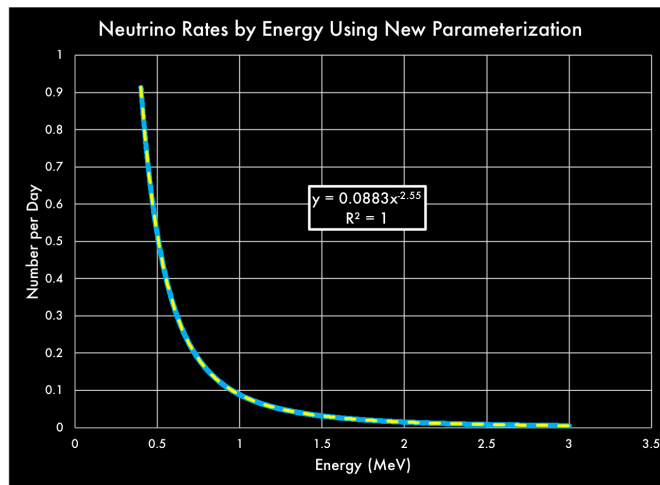


Figure 4: Results from the Monte Carlo for the neutrino energy spectrum.

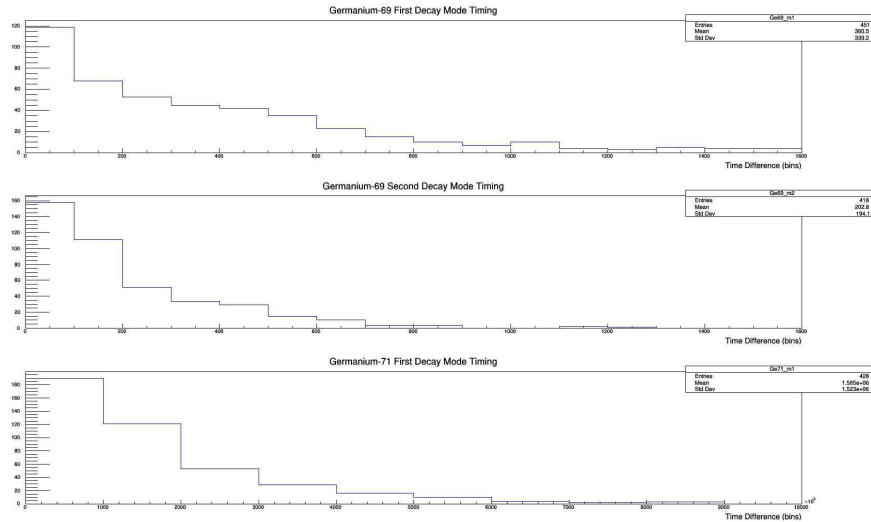


Figure 5: Decay timing plot for each germanium decay mode produced in the Monte Carlo.

Since the code has shown its ability to adequately simulate the particles which are observed by the detector, the main question meant to be answered by this simulation can be addressed: can the double-pulse signal associated with neutrino-gallium interactions be used to isolate neutrino detections from background radiation events? This is where the toy detector code results are important. After the first simulation runs conducted in June, a number of important factors became evident. First, it was expected that the detection of the relatively long lifetime germanium-71 decays could be problematic, a fact which was ultimately proved. The 20-millisecond half-life of this decay is so long that the probability of detecting imposter events increases dramatically, resulting in false detections composing well over 95% of all possible detection events. In all subsequent runs, the toy detector code was set to only look for the shorter half-life decays associated with germanium-69, a change which immediately reduced the false detection rate to the 80% level. Secondly, the early implementations used the event timing exclusively as a means of isolating the neutrino events; however, this was not a stringent enough selection criterion. To isolate the neutrino signals, there must at least be a filtering by the energy of the secondary decay product, which is easily accomplished as a result of the definite energies of the decay photons. Upon full implementation of a secondary filtering in late July, the false detection rate reduced to the 60% to 75% range.

Further improvements in the detection method required the use of filtering events by the initial energy, although such a change necessitated the implementation of a neutrino energy spectrum in the code. Of additional note were time constraints resultant of the computing technology available: the aforementioned simulations were conducted using a notebook computer with a 4 GHz, dual-core processor which could essentially run the last pre-September version of the Monte Carlo at real-time pace if 100-nanosecond binning was specified. By this point, interest had shifted to 10-nanosecond windows over periods longer than 48 hours and additional energy spectrum considerations. If implemented on the notebook computer, a simulation of seven days would have taken over seventy! By mid-September, a new 2.5 GHz, 34-core machine was installed, allowing for much longer simulations at 10-nanosecond binning. With these improvements, updates to filter the events by both initial and secondary event energies were constructed and tested. By November, the simulations could yield false event rates lower than

50%.

Throughout these tests, an important goal has been the achievement of a false event detection rate less than 20%. Though more refinements are being perfected, the detector performance achieved thus far accounts for all means which can be used to isolate neutrino-gallium interaction signals. Assuming that the 50% false event rate is a good upper-limit, the desired 20% rate is likely to be accomplished through key changes in mission parameters and detector design. All aforementioned simulations assumed a 7 solar-radii distance from the Sun and a 1% gallium dopant concentration in the liquid scintillator. Much closer distances and higher dopant concentrations may be possible, and have been considered in other trials. Conducted in early December, these trials used very rough estimates of potential improvements; however, the increase in neutrino flux at 3 solar-radii is well-founded and can be expected to give an improvement reasonably close to that found in these trials.

The fast timing Monte Carlo simulations developed over the previous eight months have resolved many technical challenges and introduced new possibilities for the proposed science instrument. Despite a potentially difficult particle environment for this detector concept, the current trajectory of continued reduction of false readings via improving event selection considerations validates the concept's proposed capabilities and justifies further development.

Detailed Detector Simulations with GEANT-IV:

A detector placed in proximity to the sun must be able to distinguish the neutrino signal from the solar and galactic background. A particle physics simulation using the Geant4 Simulation Toolkit has aimed to reduce false signals from (a.) galactic cosmic ray protons and (b.) the diffuse gamma ray background by using radiation shielding and a double pulse technique. The simulation modeled the detector and processed all of the interactions for individual background events or individual neutrino events.

A "double pulse" is being used to distinguish a neutrino event from a background event. Neutrinos interact with Gallium-69 added as a dopant to the liquid scintillator. This interaction yields an electron and an excited state of Germanium-69. This electron generates the "first pulse" of optical photons in the liquid scintillator. The excited Germanium-69 state emits a gamma ray when it decays that generates the "second pulse" of optical photons in the liquid scintillator. We look for the "first pulse" in the first 50 nanoseconds, and the "second pulse" is sought for about the next 20 microseconds.

Please note that Geant4 does not provide libraries to process neutrino interactions. Instead, we emit the final state particles of a neutrino event into the detector, and allow Geant to control any radioactive decays that may occur. Currently the best efficiency for the detection of a double pulse from a neutrino event without incorporating dead time or background is 84% for the 87 keV gamma ray, and 67% for the 397 keV gamma ray.

While individual background events should not generate such a double pulse, they can leave energy in both time windows. The elements of the detector outside of the liquid scintillator are designed to help generate secondary charged particles that a polystyrene veto detector can see prior to any signal in the liquid scintillator. Background events should hit the elements outside the liquid scintillator first, and neutrino events should start in the liquid scintillator.

The greatest challenge to the rejection of individual external background events occurs at the lowest energies for both gamma rays and cosmic ray protons. An external tungsten detector shell has been selected to maximize charge production by low energy gamma rays for better detection in the veto.

The good news is that when background events are energetic enough to leave energy in both time windows, they also leave energy in the veto before registering anything in the liquid scintillator. At current statistical levels, the program does not find any false neutrino signals from individual gamma rays or cosmic ray protons of galactic origin. Future work includes investigating whether multiple events can simulate the double pulse topology while escaping detection by the veto. Determining how often neutrino events are lost due to dead time (i.e. the time needed for a detector to process a set of particle interactions) will also be of interest.

While more mass can enhance the capture of neutrino signals and the rejection of galactic backgrounds, less mass is desired to make the orbital mechanics and the cost of a mission feasible. So optimization of mass will be necessary. One response may be to add more Gallium to enhance the detection of neutrino events, but this could reduce light collection by the photomultiplier tubes. Future simulations will need optical data for doped liquid scintillators to determine an optimal percentage of Gallium or other dopant.

The key routine in the Geant4 Simulation Toolkit is the DetectorConstruction routine. This is where one builds the detector elements, fills them with materials of interest, and places them in the world geometry. It also allows one to define volumes as sensitive detectors, which facilitates the collection and processing of information from particle physics interactions that occur in said volume.

The rest of the files in the Geant4 toolkit have unique functions, such as defining physics libraries or setting up ntuples and histograms, or writing information to said ntuples. On occasion we have written out information to a data file for examination in Excel, but nominally we use the Root analysis package to make analysis cuts and generate plots. Once the program compiles, one can run a handful of events and check to see that the geometries do not overlap because Geant will crash if it cannot assign information to a unique volume. Then one builds up the number of events in subsequent runs for sufficient statistical persistence. The user must provide a set of input files that help to control the program. For example, which physics libraries should be called, how many events are going to be run, how the detector is to be displayed, or how the initial particles are going to be fired at the detector (or in the detector). Of significance are the files that control the energy distribution for cosmic ray protons and define the optical properties of selected detector volumes.

Background particles are fired into the detector assembly from the inside of a spherical surface that is 1 meter in radius. Making that radius bigger only generates more particles that will miss the detector and waste computer time. The center of the sphere is placed at the center of the assembly.

Neutrino events should nominally come from the sun, so solar neutrinos are fired along the z-axis inside the liquid scintillator. The neutrino will be transported in Geant, but no

interactions occur. In the PrimaryGeneratorAction routine we take the energy of that neutrino and share it with the final state electron and an excited state of Germanium-69. We define the half-life of the state and the energy of the gamma ray in the same routine.

Once radioactive decay is turned on in Geant, it is turned on for everything...including the Germanium-69 ground state that has a half-life of 39 hours. We thus try to avoid collecting any information associated with this particular beta decay while studying double pulses. The assembly includes a carbon foam heat shield, a tungsten electromagnetic shield, and a gap of empty space before the main detector, which sits in the shadow of the tungsten shield. Because it is so heavy, the tungsten shield will be tidally locked and always face toward the sun. Temperatures in the shadow should be cool enough so that the liquid scintillator is not impacted by heat or radiation from the sun. Solar particles are assumed to travel along straight lines because there are no magnetic fields in the simulation.

The main detector includes a tungsten detector shell, an initial polymer shell, several small alternating layers of aluminum and polyethylene to foster charge production, a thin copper layer to aid with charge production, a polystyrene veto, and a liquid scintillator made out of mineral oil. The liquid scintillator is offset to the side farthest away from the tungsten electromagnetic shield. Currently the volume just in front of the liquid scintillator (seen as blue in Figure 1) is empty, but eventually that will be filled with electronics. In general that will impact the analysis because galactic particles can scatter off of the electronics.

The ends of liquid scintillator are in optical contact with glass disks that mimic the behavior of photomultiplier tubes. We note that the thicknesses of each material are subject to change, particularly when mass and dopant concentration are optimized. The current iteration has increased the thickness of the polystyrene veto in order to improve background event rejection.

Thin aluminum layers surround the polystyrene veto to optically isolate it from the liquid scintillator. The backs of the glass disks also have an aluminum layer to stop optical photons. Optical data files control how optical photons behave at boundaries, but if they enter a metal volume (such as aluminum), the optical photons are killed in the simulation.

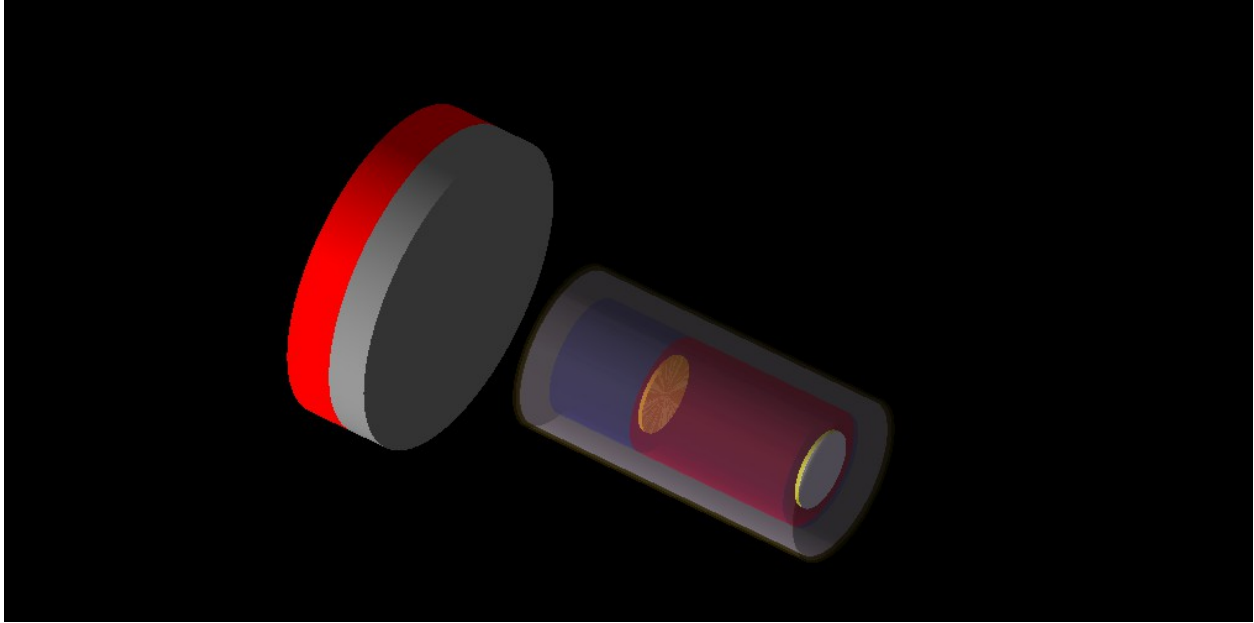


Figure 1: The NuSolar Detector

The heart of the detector is a liquid scintillator (in maroon in Figure 1 above), which we have modeled as being similar to mineral oil. Because we do not yet have the optical characteristics of mineral oil, we use the optical characteristics of a polymer called polyvinyltoluene (PVT) that has been used in previous optical studies. This will change the shape of the optical pulse that is generated and perhaps the number of optical photons that are produced. For the moment the key factor is whether optical photons make it into the photomultiplier glass for data analysis.

Geant allows one to define detector volumes as sensitive detectors, which facilitates the collection of information about all tracks that occur in the detector. The general approach will allow one to collect information like total energy deposited, total charge deposited, the number of gamma rays or neutrons that traverse the volume, etc.

However, to collect more information for each track (such as time and energy), we wrote new code for a set of our own sensitive detectors. The largest benefit of this is the access that one has to the data stack for tracks that occur inside a detector volume. The Geant4 toolkit provides a subroutine for sensitive detectors called “ProcessHits” to examine aspects of each track in the detector volume. For instance, if we find a gamma ray with an energy between 396 keV and 398 keV, we can determine when that occurred in that detector volume, and whether it was produced via a radioactive decay process, and whether the parent particle was indeed an excited Germanium-69 state.

This was also necessary to determine whether background events deposit energy in the veto prior to leaving energy in the liquid scintillator. Tracks can go through the detector volume without leaving energy, but ProcessHits will provide the time it enters or leaves the volume regardless.

The code is set up so that optical photons can be made in the liquid scintillator, the polystyrene veto, and the photomultiplier glass. In some sense, optical photons in Geant serve as an extended ray tracing exercise. Each optical photon can reflect/refract at each boundary

without loss of energy at each step. Once it has reached its attenuation length in the material, Geant kills the optical photon track.

We have not yet selected a technology for the photomultiplier tubes (or something similar), and the code is not yet set up to convert optical photons into photoelectrons. What we do instead in the simulation is use the glass disk as a placeholder, and then collect information for the optical photons as they enter into the glass. An optical photon energy pulse is developed by adding a bit of energy into the histogram bin that corresponds to the time said optical photon enters the photomultiplier glass.

Neutrino Physics

The neutrino is a neutral subatomic particle that is copiously produced in nuclear interactions. However, it does not interact very often with normal matter. That is good news for allowing us to see neutrinos coming from the sun, but a challenge for detecting them once they get into space. While there are many different kinds of potential neutrino reactions, we have chosen to study one in particular that facilitates the double pulse technique to distinguish neutrino signals from background events.

The intermediary Germanium state can occur in one of three states. The first is the ground state, which does not emit a gamma ray. The second is an m1 state that emits an 87 keV gamma ray with a half-life of 5100 nanoseconds. The third is an m2 state that emits a 397 keV gamma ray with a half-life of 2810 nanoseconds.

The electron is fired immediately at $t = 0$ nanoseconds along with an excited germanium state. The two are fired back-to-back in their respective center-of-mass frame, but the total momentum is the same as the initial neutrino's momentum. It takes a couple of nanoseconds for optical photons generated in the liquid scintillator to reach the photomultiplier tubes (see Figure 2 below).

It is up to Geant to radioactively decay the excited germanium state. While the secondary gamma ray is usually emitted much later than the electron, occasionally it is emitted just after the electron in the primary window. Currently this represents a loss of a double pulse. In the future, bin sizes will be larger than 0.5 nanoseconds, so we may not have the requisite resolution to separate the two pulses. It may indeed be the case however that background events will generate more optical photons than either the electron or the gamma ray, so that an energy cut may help capture additional neutrino events.

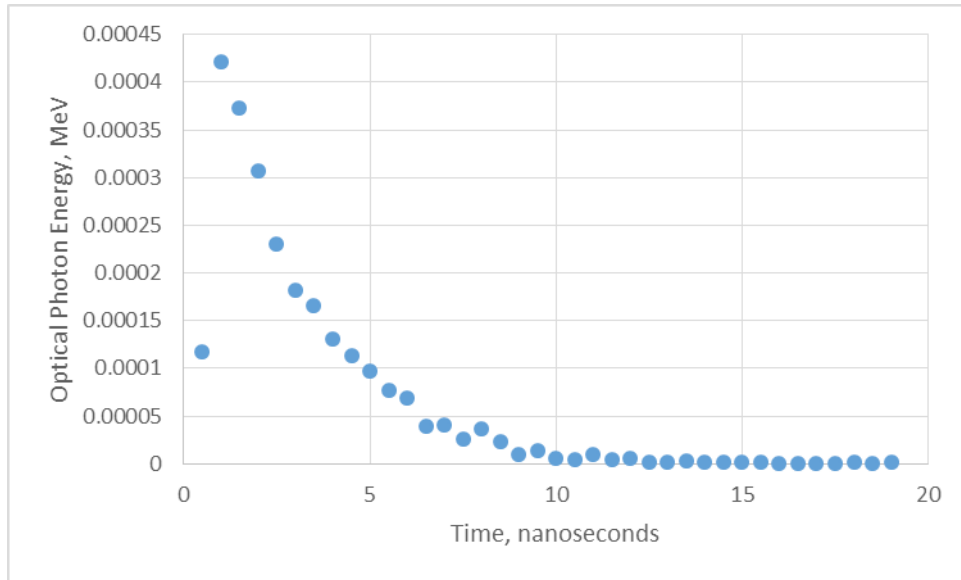


Figure 2: Example Optical Energy Pulse Reaching a Photomultiplier Tube from an Electron

In general, all pulses have a fairly short rise time, and then there is an exponential-like decay as optical photons bounce around the scintillator and make it to the photomultiplier tube glass. Above in Figure 2, the electron is emitted at $t=0$ somewhere within the liquid scintillator. Depending on where the event occurs and how it occurs, electron pulse information can extend beyond 30 nanoseconds. Future work could develop analysis cuts based upon the energy and shape of each pulse, but that may require additional data acquisition equipment. But for the moment the key piece of data is time.

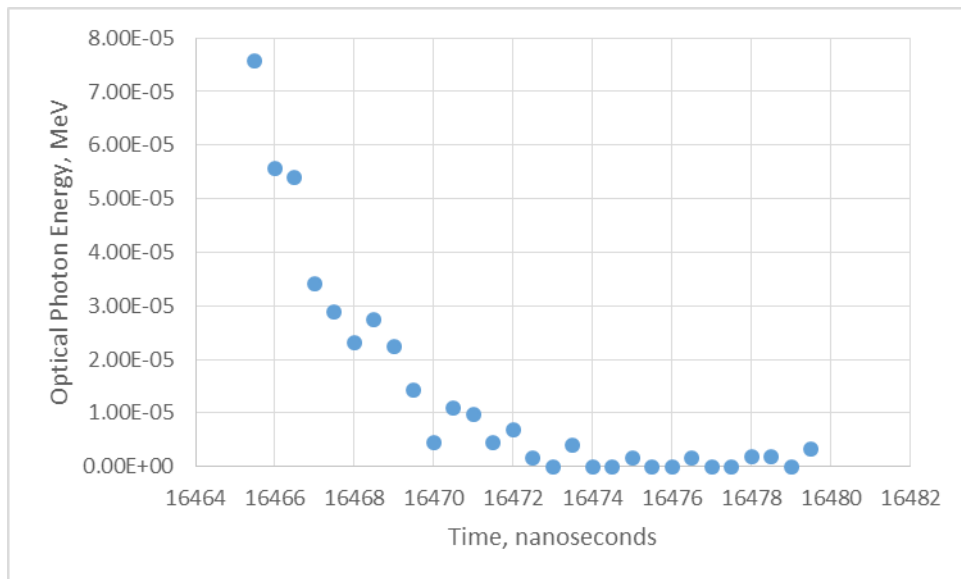


Figure 3: Example Optical Photon Energy Pulse Reaching a Photomultiplier Tube from a Gamma Ray emitted during a decay of an excited Germanium-69 state.

In Figure 3 we see a typical response of the detector to the second pulse produced by the gamma ray from a decay of the excited Germanium-69 state. Two items are noticeable when

comparing Figures 2 and 3. The magnitude of the electron pulse is larger (because the energy is larger), and the time along the x-axis is different. Gamma ray decays can occur at any time after the production of the electron.

An inefficiency for the neutrino event detection can occur due to our choice of timing cut for the primary window of 50 nanoseconds. If the secondary gamma occurs shortly after the primary electron (which happens every now and then), a double pulse is not counted. If the gamma ray decay occurs after 20 microseconds, the double pulse is not counted. Gamma rays that occur close to the boundary of the liquid scintillator do not have enough time to interact with the scintillator, and can fail to generate optical photons that reach the photomultiplier tube as a result.

Histograms like those in Figures 2 and 3 are built for both the primary time window and the secondary time window and for each photomultiplier tube (one at either end of the liquid scintillator). We collect information about total optical energy in each window, the number of optical photons that were collected, the time at which the peak of said histogram occurs, and the peak energy of said histogram.

We note here that the bin width of these histograms is smaller than one would be able to use in reality. Half of a nanosecond is too fine of a resolution for what we will actually use. The maximum efficiencies for neutrino detection so far are 84% for the 87 keV gamma ray, and 67% for the 397 keV gamma ray. But this assumes only that optical photons are found in both photomultiplier tubes, so largely this includes volume effects and how often the two pulses occur in different collection windows. Further cuts for the number of optical photons collected reduce these numbers.

In Figure 4 we see a Geant event display for a 5 MeV neutrino event that does not include all of the optical photons. We rely on separating the lower energy electron and gamma ray pulses from those typically seen in background events, which are populated by many more electromagnetic and hadronic showers.

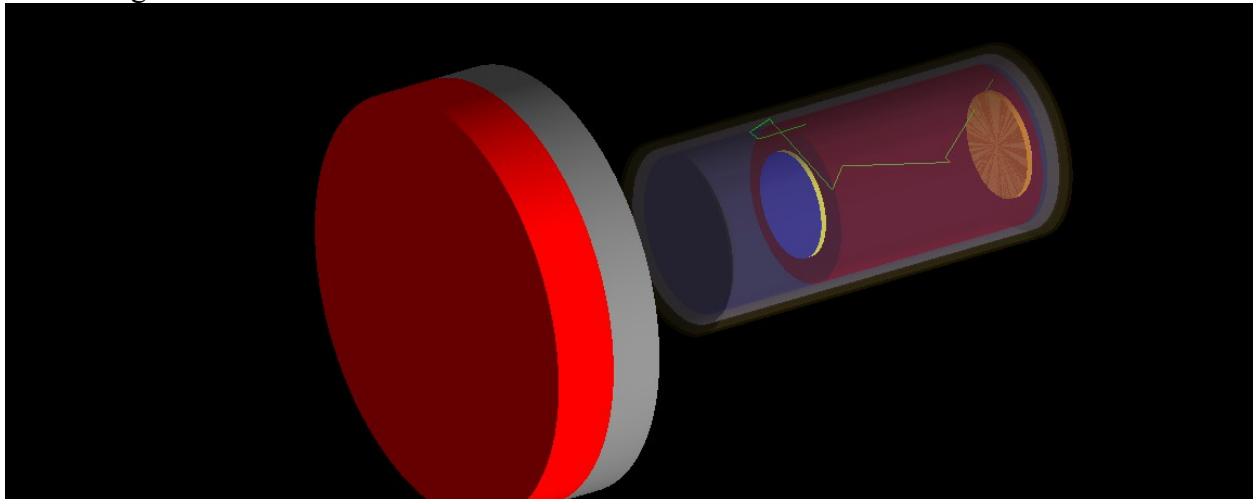


Figure 4: Sample Geant Event Display for the electron and the gamma ray in a 5 MeV neutrino event (the initial neutrino is not shown, and the optical photons are not shown).

Galactic Cosmic Ray Background

The energy spectrum for GCR protons in Figure 5 was modeled and introduced to Geant as an input data file. Geant used it as a weighted histogram to generate background particle

energies (i.e. if the bin entry is larger for a given energy, that energy should be emitted more often). The histogram is extended out to 4 TeV. Generally speaking, events with energies of several GeV and larger consume a lot of computational time. A TeV proton can generate many secondaries, and each secondary could come with hundreds of thousands of optical photons, if not more.

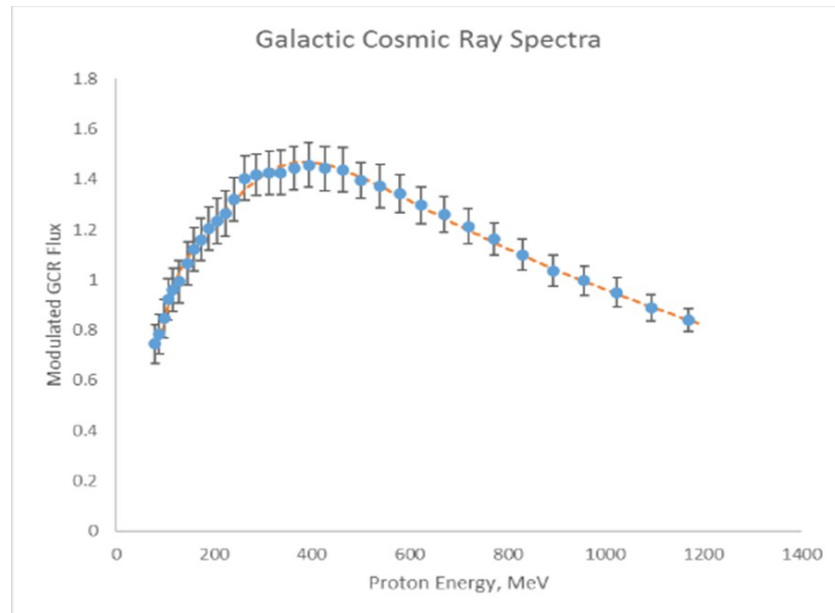


Figure 5: The Modulated Galactic Cosmic Ray Spectra

In Figures 6 and 7 below we show how successful the current veto architecture without any double pulse requirement is at rejecting cosmic ray protons. For Figure 6 we assume that there has to be at least 1 MeV of energy deposited in the veto, and a non-zero energy deposit occurs in the liquid scintillator.

In Figure 7 we only ask that there are non-zero energy deposits in both the veto and the liquid scintillator. A future cut based upon the performance of the data acquisition will lie somewhere between these curves, and these may change a little if one requires an energy cut in the liquid scintillator. This is about the best one can do...the real response will be between Figures 6 and 7 as we take into account an energy cut for the veto that is less than 1 MeV. Regardless, our design has a lower success rate when the energy of the GCR proton is lower, which means there is a greater chance of bypassing the veto and leaving energy in the liquid scintillator (which is more like a neutrino event).

Given an estimate of the rate of the GCR background, the frequency at which the veto fails, and how often the energy deposited is similar to that of a neutrino double pulse, one can estimate the rate of false neutrino signals from this background.

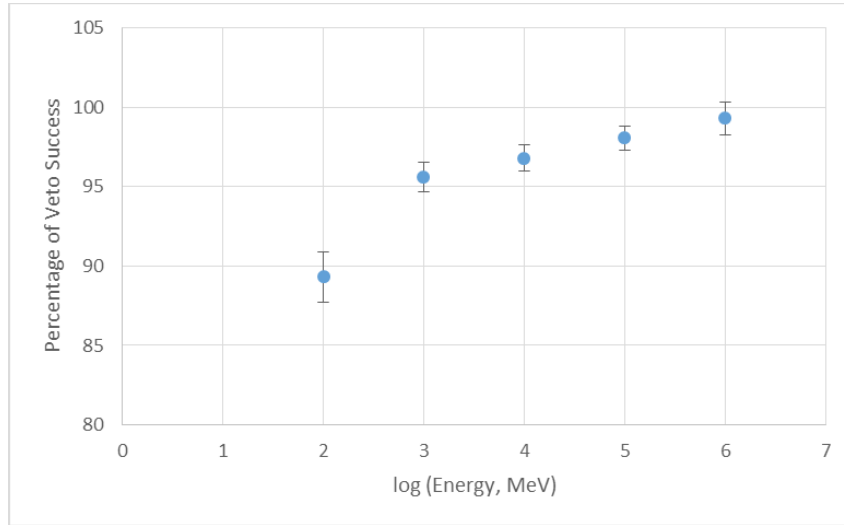


Figure 6: Veto Success Rate for Galactic Cosmic Ray Protons.
Success means 1 MeV of energy in the veto and a non-zero energy in the liquid scintillator.

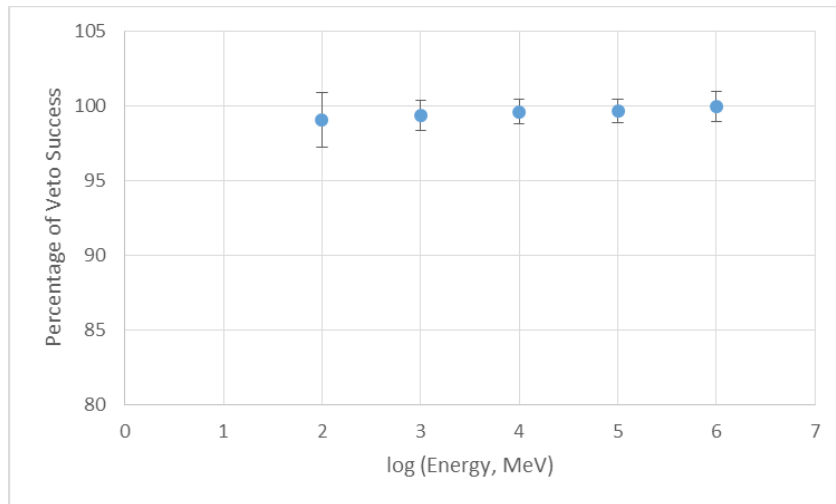


Figure 7: Veto Success Rate for Galactic Cosmic Ray Protons.
Success means both the veto and the liquid scintillator have a non-zero energy deposit.

We have improved the success rate by two methods. First, the veto is surrounded by layers of different materials. Their purpose is to facilitate the conversion of neutral particles into electron-positron pairs, since the veto needs a charged particle to generate optical photons. We see in Figure 8 that tungsten has the higher cross section for the photoelectric effect and pair production, and all materials behave similarly around 1 MeV for the Compton Effect. This not only justifies the use of tungsten for the forward electromagnetic shield, but also for the detector shell. Nevertheless, iron or steel may be a suitable substitute if mass or secondary neutrons are issues with tungsten.

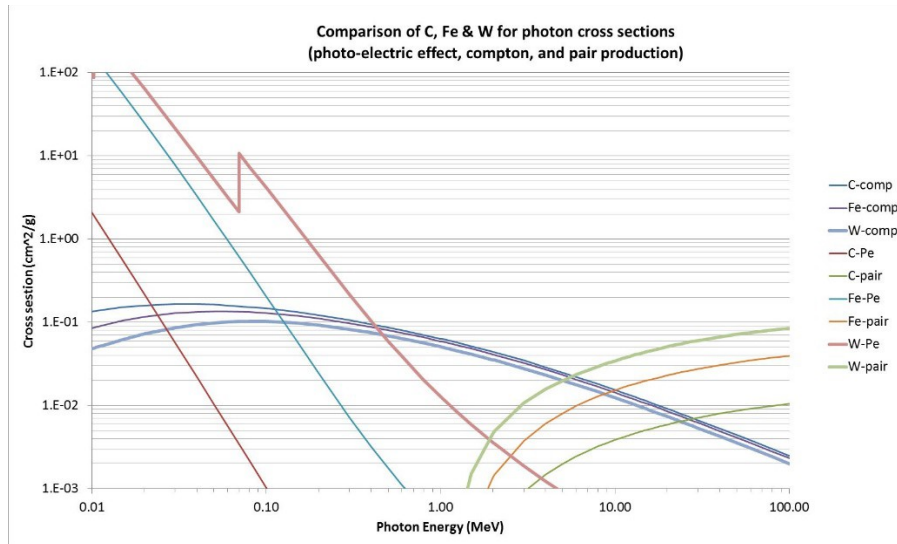


Figure 8: Cross sections for Tungsten, Iron, and Carbon for the photoelectric effect, the Compton Effect, and pair production. Tungsten has a larger cross section at both low and high energies.

Second, the polystyrene veto is 5 cm thick, which allows more time for neutral particles to interact with the polystyrene. Energy cuts, pulse shape analysis, enhanced doping of Gallium, etc. have not been fully vetted yet in an effort to reduce the thickness of the veto to save mass. The veto is currently just a solid volume, but ultimately will consist of scintillating fiber. We can also look at the response of the detector by considering the production of double pulses by GCR events. The only constraint in this regard is whether more than 5 optical photons are registered in both the primary time window and the secondary time window AND this is satisfied in both photomultiplier tubes.

We note that ultimately, one wants to generate photoelectrons to produce a current for data analysis. Roughly speaking, the current optical photon cut is a 1 photoelectron cut....which is minimal.

Figure 9 shows that the percentage of events that deposit more than 1 MeV in the veto, deposit a non-zero energy in the liquid scintillator, and satisfy the double pulse topology based on 5 optical photons increases with the log of the energy. As the initial proton energy increases, there is likely to be more spillover into the secondary window, either from secondaries or from radioactive decays. We do not imply at this point that a sharp peak occurs in the secondary window, only that energy is deposited. Such double pulses will be rejected based upon the veto.

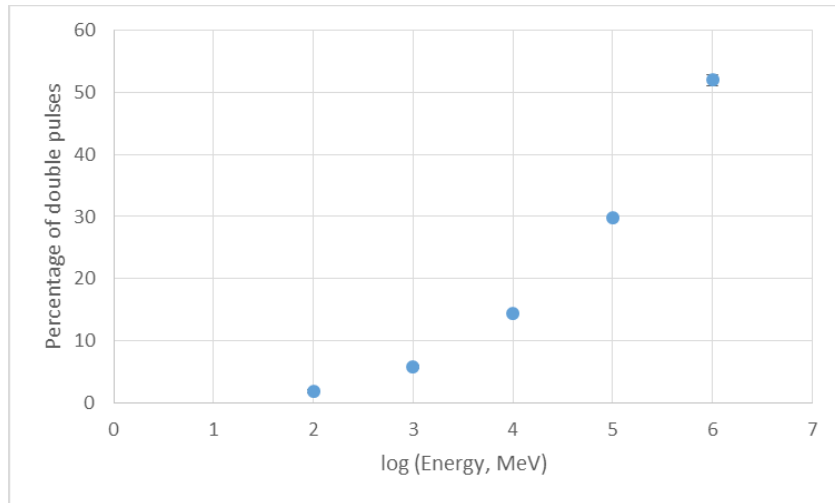


Figure 9: How often a GCR event satisfies the veto requirements of Figure 5 AND satisfies a double pulse in both photomultiplier tubes.

In Figure 10 we ask how often does an event that satisfies a 5 photon double pulse requirement also leave more than 1 MeV in the veto and something in the liquid scintillator. We see that the lower energies are more likely to fail to provide a 1 MeV energy deposit in the veto.

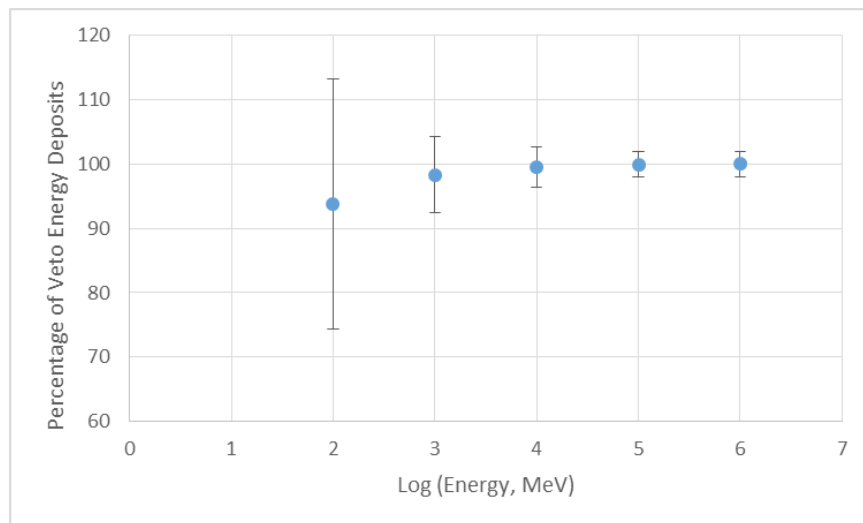


Figure 10: How often a double pulse leaves 1 MeV in the veto and something in the liquid scintillator.

Galactic Cosmic Ray protons can populate the secondary timing window in two ways to generate a “double pulse”. First, a single pulse can last longer than 50 nanoseconds and then populate the secondary window. Second, a radioactive decay initiated by the primary hadronic and electromagnetic showers can occur in the secondary window. In Figure 11 we see an example of the latter. More work is necessary to determine whether the secondary gamma in these cases is originating in the liquid scintillator or from outside the veto.

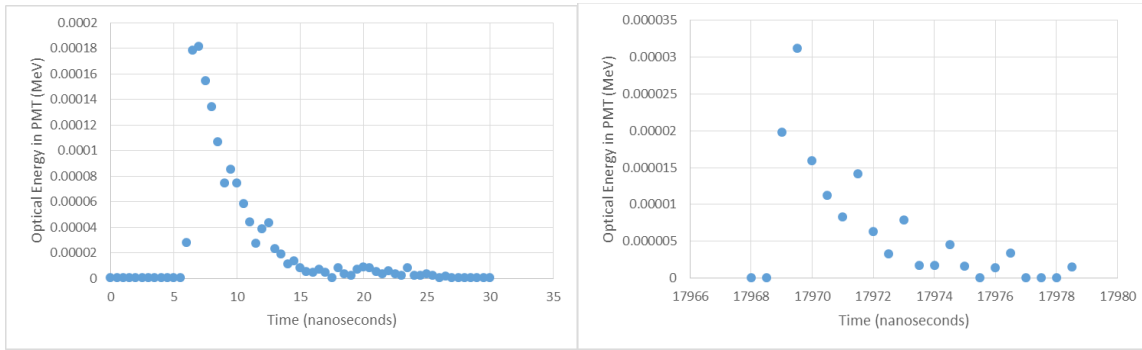


Figure 11: An initial optical photon energy deposition in the primary timing window followed by a radioactive decay in the secondary timing window. Note the scales are different.

It is also of interest to understand what Geant is actually doing via a picture from an event display. In Figure 12 below we provide a sample GCR proton event with an initial energy of 10 GeV. Geant produces all of the particles and decides when interactions occur, and then generates any secondaries as necessary.

We do not show optical photons here, because that would fill up the detector, but they would bounce around until they are stopped by attenuation or enter the photomultiplier tubes on the ends of the detector or exit the liquid scintillator. We note that further design would address things like electronics and power that have yet to be addressed.

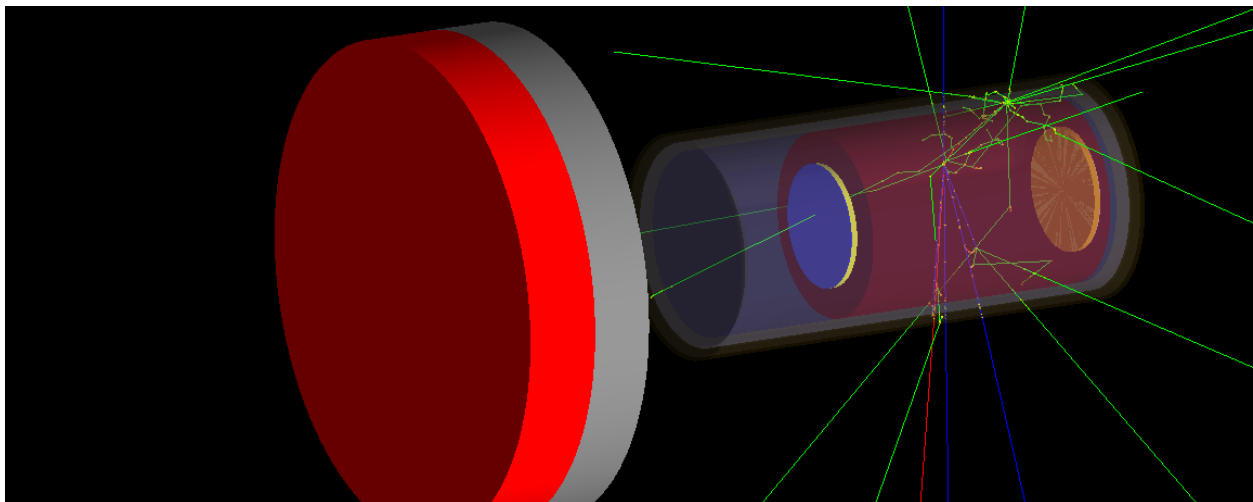


Figure 12: Sample Picture of a 10 GeV GCR proton hitting the detector.

In summary, there are more events at lower energies than there are at higher energies. At the higher energies, all of the events that produce a minimal double pulse topology also leave 1 MeV in the veto. Despite more double pulses being generated, the higher energy GCR protons can therefore be rejected individually. GCR protons with energies near 100 MeV can be rejected 90% of the time with a 1 MeV energy cut in the veto (which increases to 99% if only a non-zero energy in the veto is required). But almost none of these events generate a double pulse. Together, the veto rejects individual GCR proton events at high energies, and a double pulse requirement takes care of almost all of the low energy GCR protons.

Of interest for future studies will be the rate of multiple low energy GCR protons that do not deposit a minimum energy in the veto but leave a double pulse within the primary and secondary time windows. A cut on the energy collected or a pulse shape analysis may reduce this potential false signal further.

The caveat with regard to the statistics is that Geant4 has an upper limit on the number of events per run because the event number is stored as an integer, and runs of several hundred million events can still produce large data files. At some point, multiple runs of a billion events will need to occur to generate statistics for things like TeV particles and an assessment of dead time in the detector.

Diffuse Gamma Ray Background

The diffuse gamma ray background can be modeled with the use of a power law and an exponent of -2.31. The program currently applies such a power law between 1 MeV and 279 GeV, but this slightly overestimates the gamma ray production at the higher end. In Figure 13 we examine how often the veto architecture fails at different energies. These events deposit no energy at all in the veto, but deposit energy in the liquid scintillator. It has helped to increase the thickness of the polystyrene veto via a trial and error approach and to include additional layers to produce electromagnetic showers.

These percentages at the lower end of the spectrum have been reduced by one-half to two-thirds compared with initial studies. However, the veto does not perform as well with lower energy gamma rays as compared with lower energy GCR protons. Moreover, once a minimum energy cut is applied to the veto, the veto failure rate increases at the lower energies.

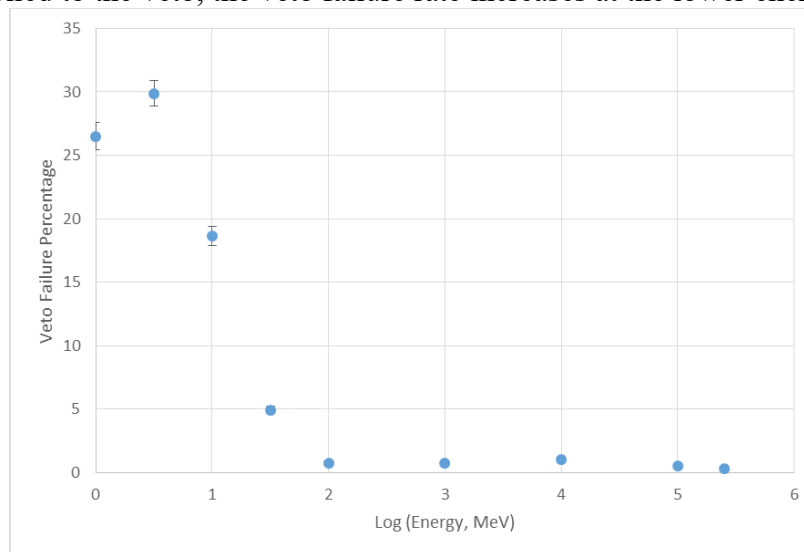


Figure 13: Rate that the gamma ray fails to deposit any energy in the veto while leaving energy in the liquid scintillator

We can also look at the behavior of double pulses as the energy increases in Figure 14 as we did previously in Figure 8. As with GCR protons, DGRB gamma rays only start to fill both primary and secondary windows at larger energies. In fact, up through 1 GeV, one does not see double pulses from gamma rays. Furthermore, this graph shows that most events that trigger a

veto response do not generate double pulses.

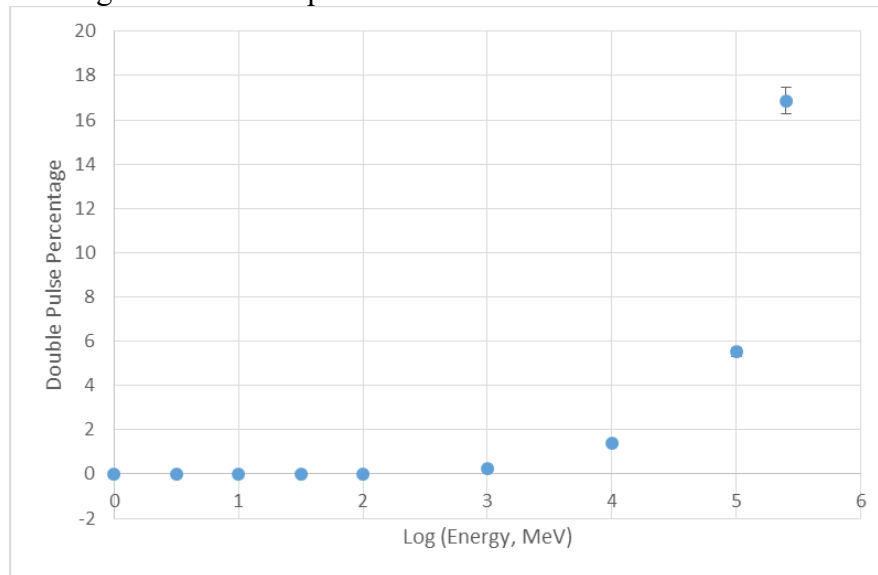


Figure 14: How often does an event that deposits more than 1 MeV in the veto and something in the liquid scintillator also satisfies a double pulse topology.

In Figure 15, we see that when we in fact do have a double pulse from an individual gamma ray event, it can be rejected based upon energy signatures in the veto about 100% of the time for energies above 100 MeV.

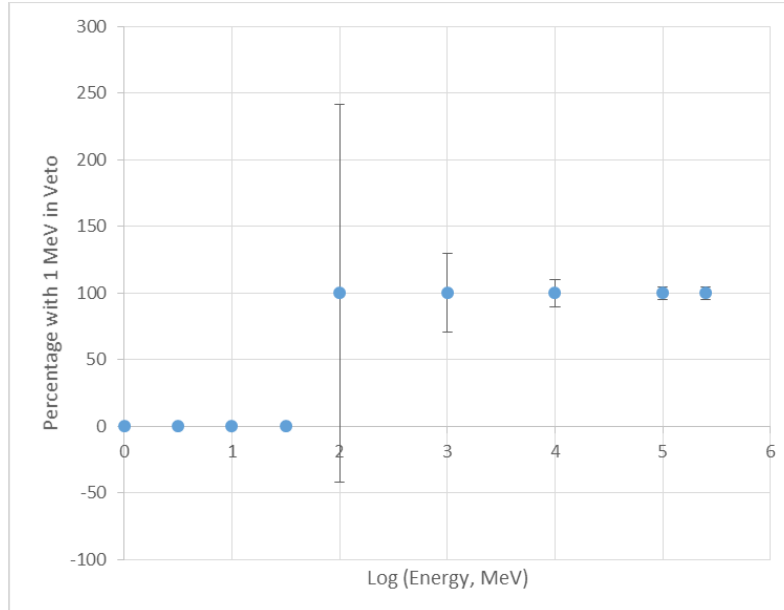


Figure 15: When we have a double pulse, how often does it leave 1 MeV in the veto?

As with GCR protons, higher energies can generate secondary pulses, and the double pulse can be generated by a very wide primary pulse and/or any radioactive decay that occurs in the secondary window.

In Figure 17 we show a typical optical photon energy deposition in a PMT for a 10 MeV gamma ray, which is one of the lower energy gamma rays that generate issues for the veto of the detector. Having several of these that fail the veto represents a challenge for double pulse recognition, which may be helped by a total energy cut.

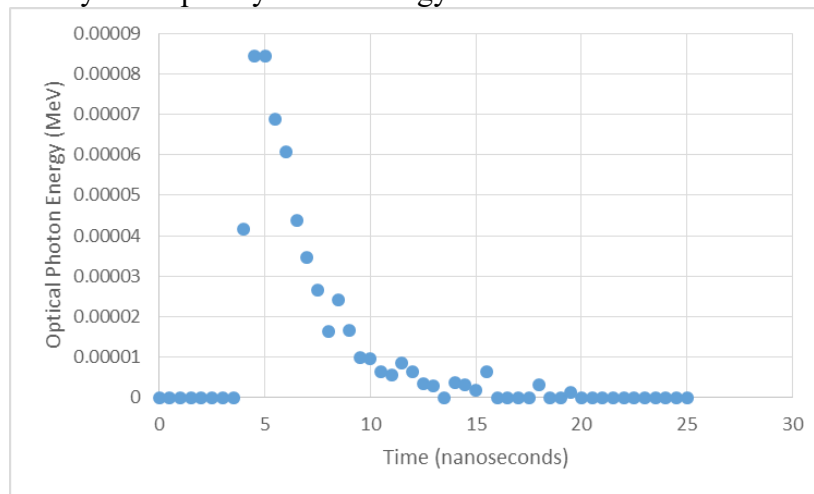


Figure 16: Optical Photon Energy Deposition in a PMT for a 10 MeV Gamma Ray

In Figure 17 one can see a typical Geant event display for a 10 GeV (not MeV) gamma ray, where one can see the shower production that can occur in the tungsten detector shell.

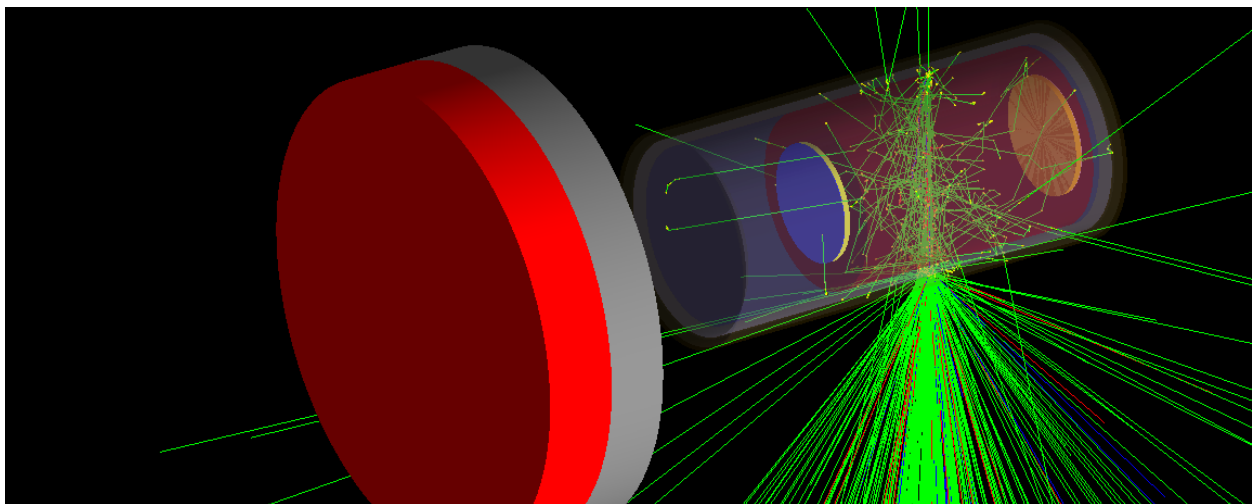


Figure 17: Sample Geant Event Display for a 10 GeV gamma ray entering through the center of the detector from above.

To summarize, at higher energies, the failure rate for the veto to trigger on DGRB gamma rays is small as it was with GCR protons. Lower energy gamma rays do not generate signals that act as double pulses.

What requires more study is the impact of multiple gamma rays at lower energies. Pulse shape and total photoelectron count in the photomultiplier tubes may help if necessary.

Rates of Background Events

Using the equation that fit the modulated GCR energy spectrum in Figure 4, we may derive the rate of certain event topologies occurring in Table 1 as

Where “F” is the number of events from the Monte Carlo that survive the applied analysis cuts. We note that one does not see a 4π in the above equation because not all of the particles are emitted toward the inside of the detector. And for this particular study we generated 100,000 events from a sphere of radius 1 meter.

The second column represents the background rate based upon energy only. It includes all events that leave nothing in the veto but something in the liquid scintillator. The third column counts all events that fail a minimum veto energy of 10 keV, but leave energy in the liquid scintillator between 1 MeV and 15 MeV. 1 MeV is close to the threshold for neutrino reactions to occur, and 15 MeV is close to the threshold of having to include neutrino interactions with Carbon in the scintillator.

Column 4 is Column 3, with an additional constraint that there are at least 20 optical photons in both photomultiplier tubes in the primary window (i.e. the first 50 nanoseconds).

Galactic Cosmic Ray Protons			
Energy (MeV)	# of Events per day • E_Veto == 0 • E_LSC > 0	# of Events per day • E_Veto < 10 keV • 1 MeV < E_LSC < 15 MeV	# of Events per day • E_Veto < 10 keV • 1 MeV < E_LSC < 15 MeV • At least 20 optical photons in each PMT in first 50 nanoseconds
100	60.0	23.08	23.08
1,000	159.2	83.50	73.06
10,000	2.75	1.37	1.27
100,000	1.09 E-02	4.36 E-03	4.36 E-03
1,000,000	1.28 E-05	8.50 E-06	7.43 E-06

Table 1: Background Rates for Galactic Cosmic Ray Protons

We note that all energies recorded collect all information available through the first 20 microseconds. We do not separately check for veto timing information against potential double pulse events (like those seen in Figure 11). In other words, we know the primary occurred from outside the veto, but did that radioactive decay occur outside the veto?

For the Diffuse Gamma Ray Background in Table 2, data was taken from a graph based on PAMELA data.

Once again, F is the number of events that survive the analysis cuts that are applied.. From <https://www.sciencedirect.com/science/article/pii/S0370157315003944> we use data for the

Diffuse Gamma Ray Background given in Figure 2.

Diffuse Gamma Ray Background			
Energy (MeV)	# of Events per day • E_Veto == 0 • E_LSC > 0	# of Events per day • E_Veto < 10 keV • 1 MeV < E_LSC < 15 MeV	# of Events per day • E_Veto < 10 keV • 1 MeV < E_LSC < 15 MeV • At least 20 optical photons in each PMT in first 50 nanoseconds
1	3.5585E+04	3.4201E+03	3.4201E+03
3.16	1.1149E+04	7.9884E+03	7.9884E+03
10	2.6818E+03	1.7915E+03	1.7915E+03
31.6	4.0329E+02	1.5075E+02	1.5075E+02
100	2.2393E+01	5.7001E+00	5.7001E+00
1000	9.7716 E-01	3.8001E-01	3.8001E-01
10000	8.2516 E-02	4.2344E-02	4.2344E-02
100000	2.5379 E-03	1.2540E-03	1.2540E-03

Table 2: Background Rates for the Diffuse Gamma Ray Background

We note that one event per second is equivalent to 8.64×10^4 events per day. So the gamma ray background rates at each energy are all less than one per second.

Future GEANT-IV Studies:

The results in Tables 1 and 2 represent an improvement from the rudimentary design that the group started with in Summer 2017. Additional shielding and production of electromagnetic showers has helped to identify background events. Further tools include optimization of the Gallium dopant and other analysis tools such as cuts on total energy and/or the shape of the pulse. Plus we need to generate photoelectrons from the photomultiplier tube, which are related to the number and energy of optical photons in the detector. Some studies will require further physical input, such a choice of photomultiplier tube, electronics for processing, and the optical data for doped liquid scintillator.

As the design progresses, changes will occur. But there will be some give and take related to the amount of mass necessary for the mission to separate background events from neutrino events, and the amount of mass necessary to deliver a payload to the appropriate orbit with enough electronics and power to operate the detector. Further studies are needed regarding the generation of secondary radioactive decays and the impact of multiple low energy particles that could simulate a double pulse event.

Future Lab studies:

With the NIAC Phase-1 studies showing a promising way to identify neutrino interactions in a high rate environment, the interest is to fabricate a test detector, tests its lab performance

with cosmic rays on the earth's surface and tagged X-rays. This would lead to a preparation for a cube-sat mission that would be able to validate the operation of the detector in space with real space background rates. This idea would fit nicely into a NIAC Phase-2 study and would also involve understanding the orbits for maximum science, launch and costs for various size probes.

References:

[1] Spitzer, L. Jr., "Report to Project Rand: Astronomical Advantages of an Extra-Terrestrial Observatory", in NASA SP-2001-4407: Exploring the Unknown, Chapter 3, Document III-1, p. 546.

[2] J. Geiseler et al., "Inner heliosphere spatial gradients of GCR protons in the low GeV range", International Cosmic Ray Conference (Rio de Janeiro 2013).

[3] R. Bonventra et al., "Non-Standard Model Solar Neutrinos, and Large Theta₁₃", 24 May (2013) arxiv:1305.5835, and Physics of the Dark Universe, Volume 4, (2014) 44-49.

[4] R. Von Ammon, "Solar Neutrino Measurement with the Radiochemical Gallium Detector (GALLEX)", Astrophysics and Space Science, Vol. 214, No. 1-2, Proceedings of the second United Nations/European Space Agency Workshop, Bogota, Colombia, 9-13 November, 1992, UN/ESA Workshops Vol. 3, p. 35-47 (1994)

[5] J. N. Abdurashitov et al., "Measurement of the Solar Neutrino Capture Rate by the Russian-American Gallium Solar Neutrino Experiment During One Half of the 22-Year Cycle of Solar Activity", Journal of Experimental and Theoretical Physics, vol. 95, issue 2, pp. 181-193 (2002)

[6] G. Alimonti et al., "Science and Technology of Borexino: a Real Time Detector for low energy Solar Neutrinos", Astroparticle Physics Vol. 16, #3, p205-234 (2002)

[7] K. Savvidy and G. Savvidy, "Spectrum and Entropy of C-systems. MIXMAX Random Number Generator", Chaos, Solitons & Fractals, vol. 91, pp. 33-38 (2016)